Pure & Appl. Chem., Vol.54, No.9, pp.1723-1732, 1982.
Printed in Great Britain.

0033-4545/82/091723-10$03.00/0
Pergamon Press Ltd.

PHOTOACTIVATION OF REMOTE FUNCTIONAL GROUPS IN ORGANIC MOLECULES AND "HOMO DICTATED" CARBONYL PHOTOCHEMISTRY

H. Morrison, A. Miller, B. Pandey, G. Pandey, D. Severance, R. Strommen and B. Bigot

Department of Chemistry, Purdue University, W. Lafayette, Indiana, 47907, USA and Laboratoire de Chimie Organique Théorique, Université Pierre et Marie Curie, Tour 44-45, 4 Place Jussieu, Paris Cedex 75230, France

Abstract - Irradiation of exo-2-benzonorbornenyl chloride and mesylate, with 254 nm light, leads to facile cleavage of the C-Cl and O-Ms groups (eq. 1 and 2). The reactions derive from the aryl excited singlet state, involve radical as well as ("hot") carbocation intermediates, and proceed more effectively with the exo, rather than endo, isomers. In the [2.2.2] series (eq. 3 and 4), fragmentation again occurs but the endo chloride is now the more reactive isomer. A new approach to rationalizing the "n,π^*" photochemistry of ketones and aldehydes is presented. The method utilizes the "HOMO dictated" nature of "$n\rightarrow\pi^*$" transformations, and is applied to the Norrish Types I and II photofragmentations (Fig. 5 and 6) and intermolecular hydrogen abstraction (Fig. 7). These Figures illustrate the use of newly developed "Delta Plots", i.e. contour diagrams which allow one to visualize the changes in electron density resulting from electronic excitation.

INTRODUCTION

The photochemical and photophysical properties of polyfunctional organic molecules continues to command intense interest, and there are now a number of known modes of intramolecular interaction between functional groups, subsequent to electronic excitation. For example, the photochemistry and photophysics of numerous non-conjugated aryl-olefins are dominated by such phenomena as intramolecular triplet energy transfer, enhanced triplet radiationless decay, singlet exciplex formation, singlet charge-transfer and di-π-methane bonding (Ref. 1). Recently, we have directed our attention to the photoinitiated cleavage of remote functional groups and have communicated preliminary observations on the photolysis of exo and endo-2-benzonorbornenyl chlorides and mesylates (Ref. 2). This paper: (1) summarizes our more recent data for these substrates, (2) presents new chemistry we have observed in the [2.2.2] bicyclic series and (3) outlines a new approach to rationalizing "n,π^*" excited state chemistry, which focuses on the "HOMO (highest occupied molecular orbital) dictated" nature of "n,π^*" primary processes. In the latter discussion, we utilize a new method ("Delta Plots") of pictorially representing the changes in charge density in different portions of a molecule produced by electronic excitation.

PHOTOINITIATED BOND CLEAVAGE IN AROMATIC BICYCLICS

Photolyses in the [2.2.1] series

Photolysis of methanolic solutions of exo-2-benzonorbornenyl chloride (1) with 254 nm light leads to cleavage of the C-Cl bond, and to the formation of products derived from both free radical and carbocation intermediates (Eq. 1). The absorption spectra of (1) and benzonorbornene (2) are

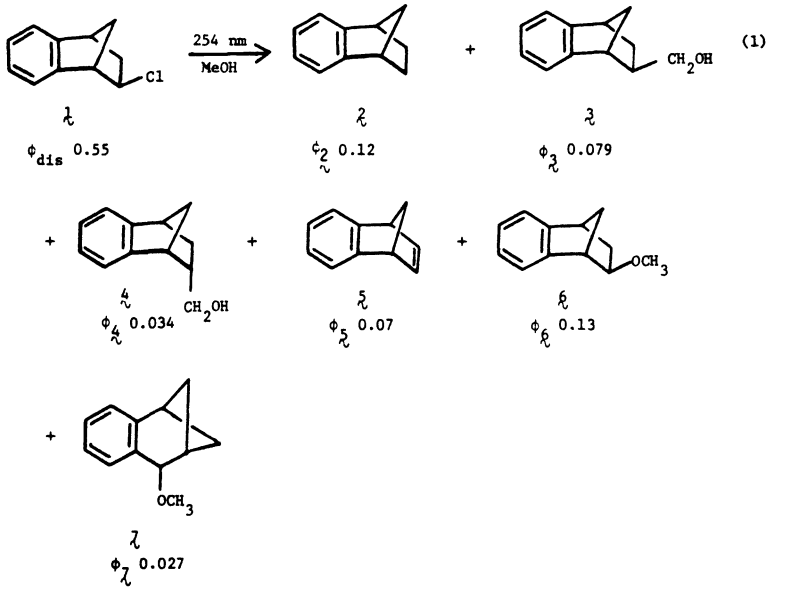

(1)

1 ϕ_{dis} 0.55 2 ϕ_2 0.12 3 ϕ_3 0.079

4 ϕ_4 0.034 5 ϕ_5 0.07 6 ϕ_6 0.13

7 ϕ_7 0.027

comparable and it may be assumed that initial excitation primarily involves the aryl $\pi\rightarrow\pi^*$ transition. A striking feature of equation 2 is the formation of the rearranged ether, 7, a product which neither we nor others have observed from the ground-state solvolysis of 1. The presence of 7 in the product mixture confirms that a "hot" (i.e. unsolvated and perhaps partially pyramidal) carbocation is generated by the aryl initiated C-Cl cleavage, much as has been observed in the direct photolysis of alkyl bromides and iodides by Kropp (3). Photolysis of exo-2-benzonorbornenyl mesylate (8) in t-butyl alcohol with 254 nm light also leads to cleavage; only carbocation derived products are observed (Eq. 2). The endo-chloride and endo-mesylate

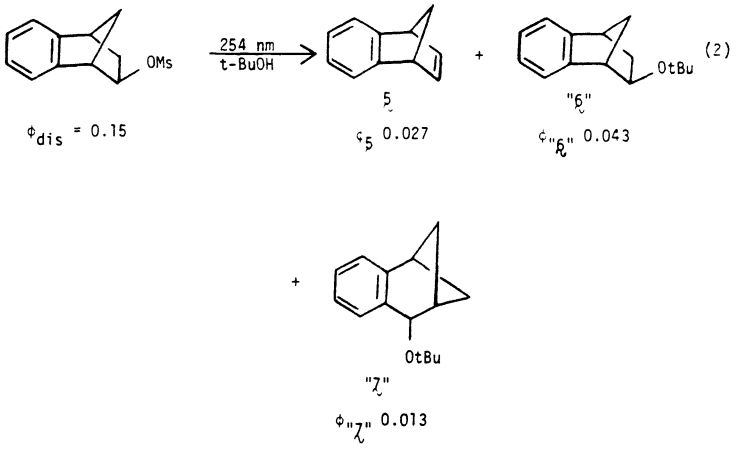

(2)

ϕ_{dis} = 0.15 5 ϕ_5 0.027 "6" $\phi_{"6"}$ 0.043

"7" $\phi_{"7"}$ 0.013

are appreciably less reactive than the exo isomers. Thus, ϕ_{dis} for the endo-chloride in methanol is 0.019, less than 4% of that observed with 1, and the endo-mesylate is virtually photoinert in t-butyl alcohol.

We have acquired appreciable evidence for the involvement of the excited singlet state in the formation of the products shown in equations 1 and 2. Our data for 1 include: (1) The insignificant quenching of 5, 6 or 7 by t-2-heptene, even though it can be demonstrated (by observing a secondary, ^{3}1* initiated di-π-methane rearrangement of 5) that the alkene intercepts an appreciable fraction of the aryl chloride triplet. The radical coupling products (3 and 4) diminish, and the benzonorbornene (2) increases, as a consequence of hydrogen abstraction from the alkene). (2) The partial quenching of ϕ_{dis} by oxygen, but only to the extent observed for ϕ_f, despite evidence (see above) that the triplets are effectively intercepted. (3) The observation that only unrearranged ether (6) is formed by p-xylene or acetone triplet sensitization. (4) An excellent correlation between substrate fluorescence and reactivity; ϕ_f for 1 in hexane is reduced by 40% relative to the endo isomer, and both ϕ_f and $^1\tau$ are reduced further in methanol. (The ϕ_{dis} of 1 is a factor of two larger in methanol than in cyclohexane). The unreactive endo isomer's emission shows no such sensitivity to solvent. Data comparable to that given above has also been obtained for the mesylate, 8.

A summary mechanistic scheme for 1 is outlined below (the substrate is denoted as R-Cl).

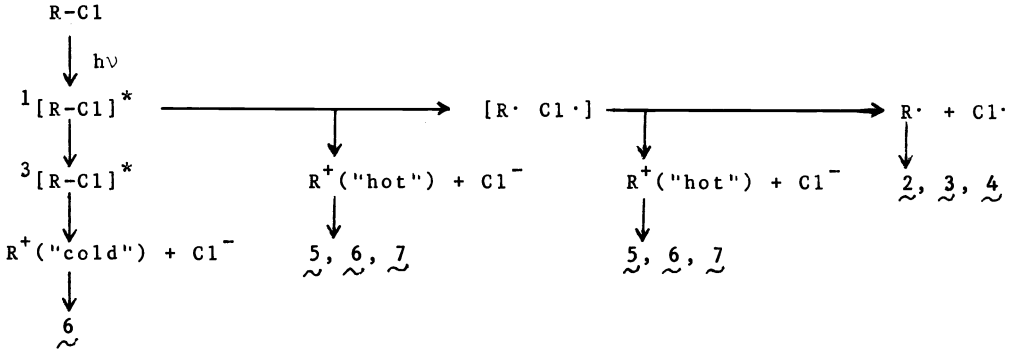

Both homolysis and heterolysis are included as sources of R^+. The homolytic pathway finds precedence in Kropp's (4) evidence that the "hot" cations formed in the photolysis of bromides and iodides are produced by electron transfer within a caged radical-pair. We observe that the use of a better hydrogen atom donor as solvent (i.e., i-propyl alcohol) increases the overall efficiency of formation of products derived from R·, with a concomitant decrease in those derived from R^+. The trend is reversed in t-butyl alcohol and we interpret these data as indicating that at least some portion of R^+ is formed from R·. However, competitive direct heterolysis of ^{1}[R-Cl]* is also implicated by the large effect of solvent polarity on the fluorescence efficiency and lifetime, and this step is therefore included in the Scheme. (A single, homolytic fission to a highly polarized radical pair is an attractive alternative mechanism which eliminates the need for two modes of C-Cl cleavage).

Exactly how the C-Cl or C-OMs bonds become activated by 254 nm excitation remains unclear. Cristol has suggested full electron transfer from the aromatic π,π^* state to the C-Cl σ^* orbital to explain the photochemistry of analogous bicyclics studied in his laboratories (Ref. 5). Our estimates of

the ΔG for this process, using the Weller equation (Ref. 6), suggest that it might indeed be thermodynamically favorable. An alternative approach is a $\pi,\pi^*/\sigma,\sigma^*$ state interaction which our calculations suggest would be appreciable. Such an interaction would lead to an avoided crossing of these surfaces and allow a correlation of the π,π^* state with [R· Cl·]. The interaction is calculated to be greater when the substituent is in the anti position and thus this approach predicts the observed stereoelectronic effects.

Photolyses in the [2.2.2] series

In fact, neither of the above analyses appear to anticipate what we have more recently observed in the benzobicyclo[2.2.2]octa-5-ene series. The photochemistry of endo-2-chlorobenzobicyclo[2.2.2]octa-5-ene (9), upon irradiation in methanol, is presented in equation 3. The product

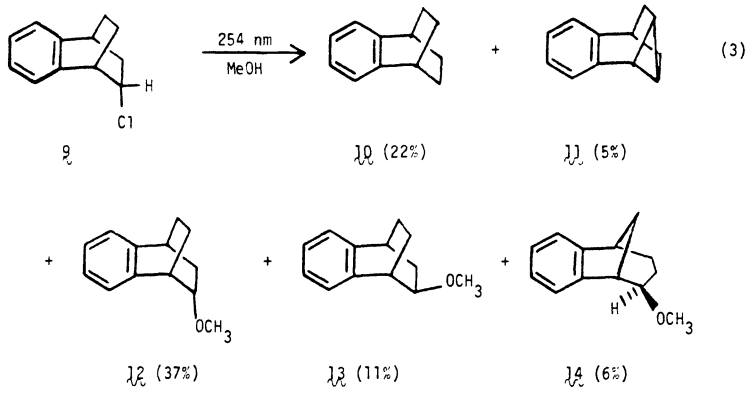

9 → 10 (22%) + 11 (5%) + 12 (37%) + 13 (11%) + 14 (6%) (3)

percentages are calculated by vpc assuming identical response factors; there is one other significant (8%), as yet unidentified, product. The rearranged ether (14) and the cyclopropane (11) are presumably formed from a hot carbocation though isotopic labelling experiments to rule out a carbene precursor to 11 are in progress. The product mixture from photolysis of the exo chloride (15) is less complex (cf. Eq. 4). The unexpected observation in

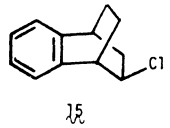

15 $\xrightarrow[\text{MeOH}]{254\text{ nm}}$ 12 (53%) + 13 (34%) + 14 (13%) (4)

this series is the inversion of the exo/endo reactivity ratio; by contrast with the factor of 25 favoring exo in the [2.2.1] substrates, there is now a ca. 5 fold enhancement of endo over exo. (Rate factors for the set of 4 substrates are: endo [2.2.1] (1.0); exo [2.2.2] (2.5); endo [2.2.2.] (12.5); exo [2.2.1] (25.0)). As in the [2.2.1] series, fluorescence efficiencies reflect the relative reactivities, so that ϕ_f for 9 is ~10% that for (15) (in methanol).

"DELTA PLOTS" AND "HOMO DICTATED" CARBONYL PHOTOCHEMISTRY

"Delta Plots" - a new way to visualize electronic excitation

These observations on the photoinduced cleavage of remote functional groups illustrate the need for new theoretical approaches to aid in our understanding of the excited state properties of polyfunctional molecules. Towards these ends, we have developed a computational and plotting sequence which creates what we have termed "Delta Plots, "i.e. contour plots which permit one to visualize the changes in electron density in different parts

of a molecule caused by electronic excitation. The sequence involves (1) calculation of the ground and excited state wave functions, using the CNDO/S-CI program of Del Bene and Jaffé (Ref. 7), (2) renormalization of the molecular orbital coefficients using a Lowdin transformation, (3) subtraction of S_o from S_1, using all the contributing one-electron excitations, to provide any net increase or decrease in electron density resulting from promotion to the excited state and (4) a plot of the molecule showing the changes in charge density. The plotting routine is essentially that developed by Jorgensen and Salem (8), modified so that net increases and decreases in electron density are depicted by solid and dotted contours respectively. A similar approach has been taken by Huber and Adams (9) wherein "electron density mapping diagrams" are used to represent the changes in electron density associated with a specific one electron transition. The overall objective of our "Delta Plots" also finds analogy in the "Δp matrices" created by Zimmerman (10). Two examples of "Delta Plots" are presented in Figures 1 and 2 for the $S_o \rightarrow S_1$ ($\pi \rightarrow \pi^*$) transition in ethylene and the $S_o \rightarrow S_1$ ($n \rightarrow \pi^*$) transition in formaldehyde, respectively. Figure 1 quite nicely pictorializes the shift of electron density from the region between the carbons to the ends of the π system, characteristic of the promotion from a π bonding orbital to a π^* antibonding orbital. Likewise, in figure 2 we see the large loss in electron density at the oxygen p_x orbital with a corresponding increase in the π system (more heavily concentrated at the carbon).

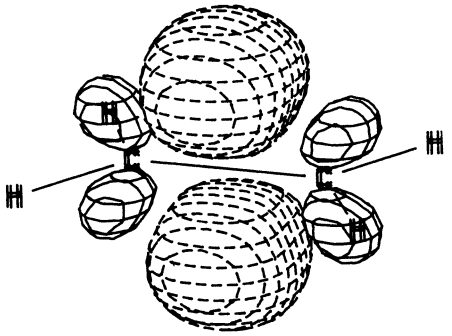

Fig. 1. A Delta Plot of the $\pi \rightarrow \pi^*$ transition in ethylene.

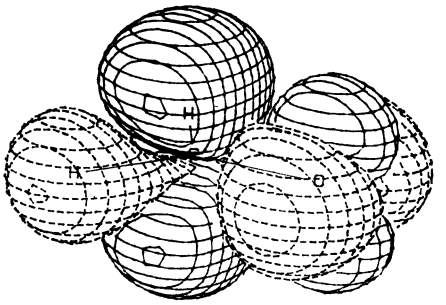

Fig. 2. A Delta Plot of the $n \rightarrow \pi^*$ transition in formaldehyde.

"HOMO dictated" carbonyl photochemistry

One of the more striking features of Figure 2 is the large loss in electron density at the C-H bond which accompanies the formaldehyde $n \rightarrow \pi^*$ transition. Delocalization of a carbonyl "n" orbital is well recognized (Ref. 8, 11), while the π^*_{CO} orbital is primarily localized at the C-O bond (cf. Figure 3). It is thus reasonable that in a so-called "$n \rightarrow \pi^*$" transition, electron density will be drained from those (non C-O) regions in the molecule which make significant contributions to the "n" orbital. Clearly, the term "$n \rightarrow \pi^*$" transition is misleading, and in simple ketones and aldehydes having a delocalized "n" orbital as the highest occupied molecular orbital (HOMO), one can only fully appreciate the consequences of $S_o \rightarrow S_1$ excitation by thinking in the more general terms of a HOMO-LUMO transition. Thus, if one examines the HOMO and LUMO of acetaldehyde (Figure 4), one notes again the large potential loss in electron density at the alpha C-H and C-C bonds upon excitation to S_1, and a Delta Plot for $S_o \rightarrow S_1$ is presented in Figure 5. It

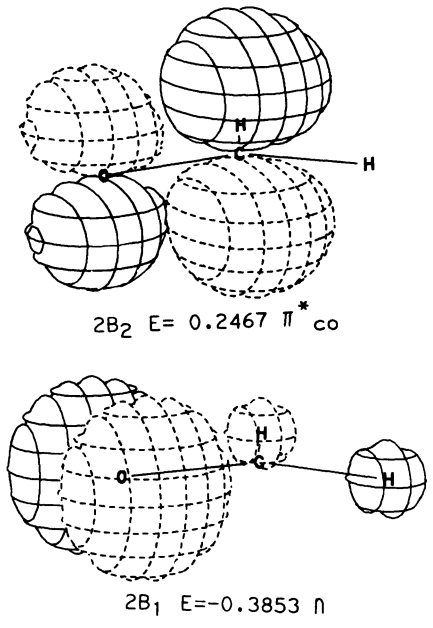

Fig. 3. The HOMO and LUMO of formaldehyde (see Note a)

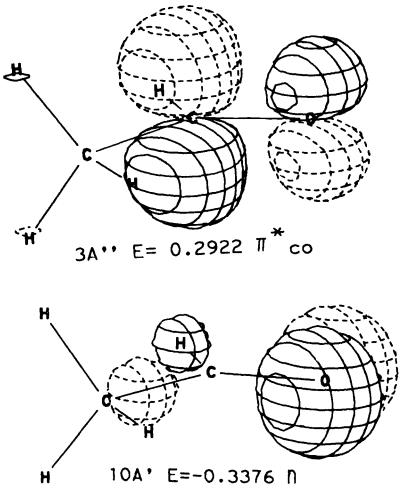

Fig. 4. The HOMO and LUMO of acetaldehyde (see note a)

is immediately evident from this Figure that one can nicely rationalize the classic Norrish Type I cleavage of the electron depleted alpha C-C bond (Ref. 12). Viewed in this fashion, the Norrish Type I cleavage may be thought of as "HOMO dictated" photochemistry, (i.e., it is its participation in the delocalized HOMO which makes the alpha C-C bond susceptible to cleavage). Note that the $S_o \rightarrow S_1$ transition in ketones and aldehydes is particularly "clean" in that the CNDO/CI calculations indicate the HOMO-LUMO one-electron excitation comprises ~98% of S_1. This, plus the localized nature of the LUMO, make an examination of the HOMO particularly informative; the Delta Plot is useful but not essential to applying the concept of carbonyl "HOMO dictated" photochemistry. (Delta Plots should be most useful where several one-electron transitions contribute to an excited state).

We believe that the concept of "HOMO dictated" carbonyl photochemistry may well be capable of rationalizing most, if not all, of the known ketone and aldehyde primary processes. We illustrate with two additional related examples: the Norrish Type II reaction and intermolecular hydrogen abstraction. Figure 6 is a Delta Plot for butyraldehyde with the molecule arranged in the chair-like geometry expected for the intramolecular Type II transition state. Standard geometrical parameters (Ref. 13) were used, with the O/γH distance equal to 1.79A°. (In the transition state as calculated

Note a. The wave functions are from extended Huckel calculations and have been plotted as in Ref. 8. We are grateful to Prof. William Jorgensen for providing us with these plots. Note that these M.O. plots use solid contours where the wave function is positive and dotted contours where the wave funtion is negative. The m.o. plots should not be confused with the Delta Plots which have been explained in the text.

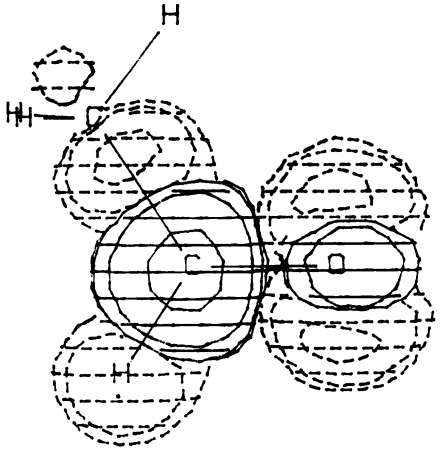

Fig. 5. A Delta Plot of the HOMO-LUMO ("$n \rightarrow \pi^*$") transition in acetaldehyde.

by Dewar and Doubleday (14), the O/γH distance is 1.60 A^{o} at which distance the molecular orbital mixing (see below) will be even greater). The loss of electron density from the (reacting) C-H bond is clearly evident in the Figure. Note that the Type II reaction contrasts with the situation which typically prevails for the Type I cleavage, in that the latter does not require a significant change in the ground state geometry. The gauche and anti ground state butyraldehyde conformers must rotate into the cyclic

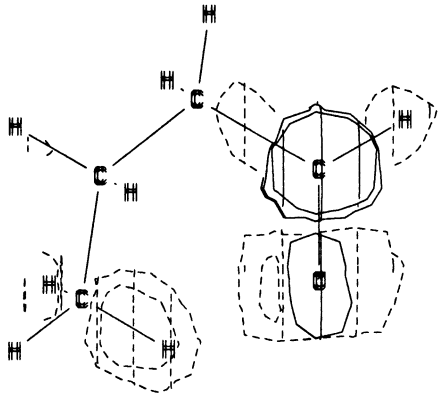

Fig. 6. A Delta Plot for HOMO-LUMO excitation of butyraldehyde in a chair geometry approximating that of the Norrish Type II reaction.

transition state after excitation in order for Type II abstraction to occur. Thus, our Delta Plot represents the flow in electron density caused by electronic excitation when the geometry approximates the transition state, rather than the initial (i.e. Franck-Condon) excited state. (A calculation on the anti conformer confirms the absence of H involvement in the HOMO at this geometry). Though Figure 6 derives from a CNDO/S computation, an analogous picture emerges with wave functions from MNDO or STO-3G calculations.

It is not surprising that photochemically induced intermolecular hydrogen abstraction (exemplified by the interaction of formaldehyde with methane) is also predicted by a Delta Plot (cf. Figure 7). An O/H distance of 1.79A^{o}

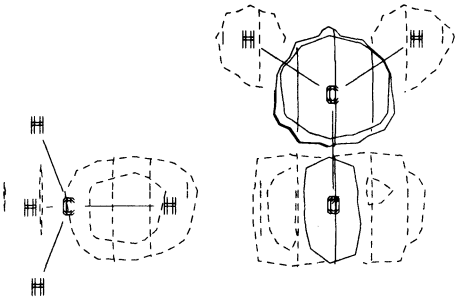

Fig. 7. A Delta Plot for HOMO-LUMO excitation of formaldehyde and methane.

was used for Figure 7, identical with that employed in the butyraldehyde calculation. One again notes the loss in electron density evident in the reacting C-H bond. A more detailed examination of the molecular orbitals for methane, formaldehyde and the interacting pair reveals the source of the HOMO involvement of the C-H group. As the methane approaches the formaldehyde, one of the π_{CH_4} orbitals interacts with both the (n_o + π_{CH_2}) and (n_o - π_{CH_2}) formaldehyde orbitals (Figure 8). This leads to a partial

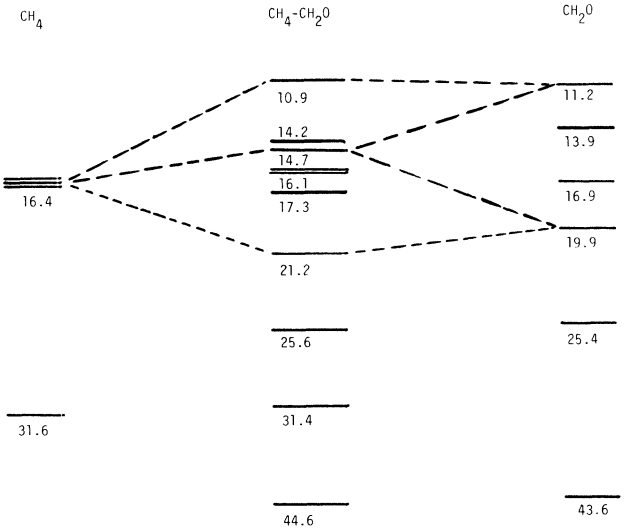

Fig. 8. Molecular orbital interaction diagram for formaldehyde and methane.

mixing (ca. 11%) of the π_{CH_4} orbital into the formaldehyde HOMO (Figure 9) (as usual, the LUMO is essentially unperturbed). Clearly, this analysis

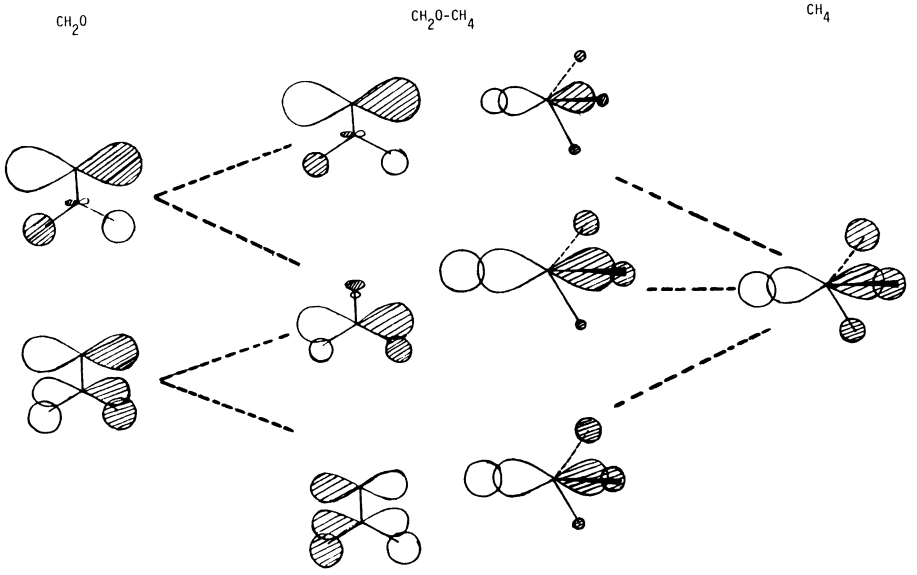

Fig. 9. The principle mixing of molecular orbitals for methane and formaldehyde.

lends itself to an examination of hydrogen abstraction as a function of O/H distance, stereoelectronic effects (i.e. C/O/H bond angle and H/C/O/H dihedral angle), substituent effects etc.; such studies are in progress. We are also extending the concept of "HOMO dictated" photochemistry to the other primary processes characteristic of ketones and aldehydes, as well as to other functional groups reacting via "n,π^*" states. One may look upon the butyraldehyde Type II reaction as chemistry resulting from a "bifunctional" interaction between the carbonyl and C-H units. In this vein, we expect the HOMO and Delta Plot analyses will be equally useful for predicting photoactivation of remote functional groups in molecules such as amino- or chloroketones. Theoretical and experimental studies of such systems are in progress.

Acknowledgements - This work was supported by a grant from the National Science Foundation (CHE-7926499). We are grateful to Prof. William Jorgensen for the considerable assistance and encouragement he has provided in the development and interpretation of the Delta Plot analyses.

REFERENCES

1. H. Morrison in Organic Photochemistry (A. Padwa, Ed.), Volume 4, pp. 143-189, Marcel Dekker, New York, (1979).
2. H. Morrison and A. Miller, J. Am. Chem. Soc., 102, 372-373 (1980).
3. P. J. Kropp, J. R. Gibson, J. J. Snyder and G. S. Poindexter, Tetrahedron Lett., 207-210 (1978), and references therein.
4. P. J. Kropp, G. S. Poindexter, N. J. Pienta and D. C. Hamilton, J. Am. Chem. Soc., 98, 8135-8144 (1976).
5. S. J. Cristol, R. J. Opitz, T. H. Bindel and W. A. Dickenson, J. Am. Chem. Soc., 102, 7978-7979 (1980) and references therein.
6. D. Rehm and A. Weller, Isr. J. Chem., 8, 259-271 (1970).
7. J. E. Del Bene and H. H. Jaffé, J. Chem. Phys., 48, 1807-1813 (1968); R. L. Ellis, G. Kuehnlenz and H. H. Jaffé, Theor. Chim. Acta, 26, 131-140 (1972).
8. W. L. Jorgensen and L. Salem, The Organic Chemist's Book of Orbitals, Academic Press, New York (1973).

9. J. R. Huber and J. E. Adams, (Ber. Bunsenges Phys. Chem., 78, 217-223 (1974).
10. See, for example, H. E. Zimmerman, M. G. Steinmetz and C. L. Kreil, J. Am. Chem. Soc., 100, 4146-4162 (1978); H. E. Zimmerman and R. E. Factor, Tetrahedron, 37, Supp. No. 1, 125-141 (1981) and references therein.
11. For example, A. V. Luzanov, Russ. Chem. Rev., 49, 1033-1048 (1980).
12. The importance of the HOMO for Norrish Type I photoreactivity is discussed in B. Bigot, A. Devaquet and A. Sevin, J.C.S. Faraday II, 76, 1234-1244 (1980).
13. J. A. Pople and M. Gordon, J. Am. Chem. Soc., 89, 4253-4261 (1967).
14. M. J. S. Dewar and C. Doubleday, J. Am. Chem. Soc., 100, 4935-4941 (1978).